

# Production Optimization Using Bean Size Selection for Niger Delta Oil Wells

Idongesit Effiong Essen<sup>1</sup>, Dulu Appah<sup>2</sup>, Mfon Godwill Udoaka<sup>3</sup>

<sup>1,3</sup>Department of Petroleum Engineering, University of Uyo, Uyo, Akwa Ibom State, Nigeria

<sup>2</sup>Department of Petroleum and Gas Engineering, University of Port Harcourt, Choba, Rivers State, Nigeria

---

**Abstract:** The oil and gas production system requires energy in the form of pressure, and the choke plays an important role in controlling the flow rate. In this work, Nodal Analysis method was used to optimize oil production using bean size selection for two wells B40 and B50, respectively. PIPESIM was used to build the models for the two wells using the test production data acquired. For well B40, when there is bean-up from 0.2" to 0.8", flow rate increases from 363.957STB/D to 2132.306STB/D at bottomhole and 359.535STB/D to 1890.471STB/D at wellhead nodes, respectively. For well B50, when there is bean-up from 0.2" to 0.8", flow rate increases from 195.648STB/D to 4464.972STB/D at bottomhole and 500.005STB/D to 3870.941STB/D at wellhead nodes, respectively. This is evident in the plots whereby the operating point shifts repeatedly to the right as the bean size is increased successively. Finally, at the end of the study, the bean size for well B40 was re-selected from 0.25" (1/4) at a flow rate of 605.171STB/D to 0.28" (17.92/64) at a flow rate of 728.019STB/D. Similarly, for well B50, the initial bean size prior to optimization was 0.4" (25.6/64) and the flow rate was 1962.357STB/D. However, a bean-up to 0.5" (1/2) produced at a flow rate of 2882.492STB/D thus production optimization is achieved.

**Keywords:** Optimization, Bean size, Flow rate, Wellhead pressure, Gas-oil ratio, Nodal Analysis.

---

## 1. INTRODUCTION

The oil and gas production system comprises of flow of hydrocarbon fluids from the reservoir to the surface production facilities through the production tubing. It include inflow performance (flow from the reservoir into the wellbore), as well as outflow performance (flow across the down-hole completion and restriction, safety valve, and up the tubing string to the surface facilities).

In practice, all flowing wells make use of some surface restrictions in order to regulate the flowing rate. Only very few wells are produced with absolutely no restrictions for getting maximum production rate [1]. The overall performance of a production well is a function of several variables. Examples of these variables are tubing size, choke size, flow line size, and perforation density. The flow rate (Q) is a measure of the rate at which a reservoir fluid is produced and is a function of the perforation density, reservoir pressure, tubing size, choke/bean size, diameter of flow-line, and separator pressure [2]. This implies that changing any of these variables will alter the performance of the well.

Surface or wellhead chokes are utilized in the oil and gas industry to regulate the flow rate so as to maintain well allowable, to protect surface equipment, to prevent water and gas coning, and to provide the necessary backpressure to avoid formation damage due to excessive drawdown [3].

There are numerous oil and gas wells around the world that have not been optimized to achieve the desired flow rate. The implication is that the wells are not produced at the most efficient rate (MER). At times, large amounts of money have been wasted on stimulating the formation when the well's producing capacity was actually being restricted because of wrong choice of bean size. Implications of small bean size include low flow rate, unstable flow, and high gas-oil ratio (HGOR).

Another source of error in completion design is the installation of chokes/beans that are too large. This often happens on wells that are expected to produce at high rates. Increased well performance can be achieved by larger bean size on the wellhead. A bean size that is too large can actually increase the rate at which a well will flow, but if not properly monitored, will result in high pressure drawdown which causes sanding and water production. This can also cause liquid load up which leads to early depletion or eventual death of the well. In fact, many wells have been completed in this manner and their maximum potential rate could not be achieved.

The first theoretical investigation on two phase flow across chokes was performed by [4]. However, this theory can be useful when the phase is continuous and the gas liquid ratio is lower than one [4]. In 1960, a new theory based on Tangren's theory was proposed by Ros for a continuous gas phase. This analysis led to the development of an equation relating mass flow of gas and liquid, upstream pressure and choke size [5]. To make Ros' correlation available to oil field workers, Poetmann and Beck converted the correlation to oil field units and reduced it to a graphical form [6].

In 1969, Omana, Brown, Brill and Thompson conducted experimental field tests at the facilities of Union Company of California's Tiger Lagoon Field in Louisiana to study the multiphase flow of gas and liquid (gas-water system) through a small-sized choke in a vertical position, and used dimensional analysis to obtain their empirical equation [7]. In 1975, a theoretical model relating dynamic orifice performance in both critical and sub critical flow regimes was developed [8].

Many empirical equations have been developed to estimate the relationship between production rate and wellhead pressure for two-phase critical flow. The first empirical correlation for choke selection was done by Gilbert in 1954. He developed an empirical correlation for critical flow through a choke. He used production data from flowing oil wells in the Ten Section field of California [9]. Gilbert's equation consists mainly of a three parameter equation in which the flow rate is linearly proportional to the upstream pressure.

$$P_{WH} = \frac{10q_l R^{0.546}}{S^{1.89}} \quad (1)$$

Where  $q_l$  is liquid production rate (bbl/day)

R is gas liquid ratio (SCF/STB)

$P_{WH}$  is the well or tubing head pressure (psig)

S is the bean size (1/64) inch

The second experimental relation was proposed by Baxendell in 1957. He revised Gilbert's equation to update the coefficients based on incremental data [10]. The revised equation of Baxendell is given by:

$$P_{WH} = \frac{9.55q_l R^{0.546}}{S^{1.93}} \quad (2)$$

The third experimental relation was proposed by Achong in 1961. He modified Gilbert's equation to match the performance of wells in Lake Maracaibo field in Venezuela [11]. The rate of multiphase flow through a choke, and the upstream pressure are, according to Achong, correlated by the following relationship:

$$P_{WH} = \frac{3.829q_l R^{0.65}}{S^{1.88}} \quad (3)$$

Omana, Brown, Brill and Thompson carried out some experiments in the Tiger Lagoon field of Louisiana by using natural gas and water flowing through restrictions [7]. In 1972, Fortunati introduced two correlations for subcritical and critical flow through chokes [12].

In 1975, Ashford and Peirce developed a mathematical model relating dynamic orifice performance in both critical and subcritical flow regimes [8]. In 1986, Sachdeva, Schmidt, Brill and Blais developed a model to calculate flow rate of a choke by investigating a two-phase flow through wellhead chokes, including both critical and subcritical flow [13]. Ajenka and Ikoku analysed several correlations, including those by Gilbert, Baxendell, Ros, Achong, and Ashford, and proposed two well models [1], [14].

In 1996, Elgibaly and Nashawi developed a correlation to describe the choke performance of the Middle-East oil wells [15]. In 2007, Ghareeb and Shedid attempted to overcome the limitations of the existing correlations for artificially flowing wells by developing a new correlation capable of calculating precisely the wellhead flow production [16]. In 2007, Alrumah and Bizanti used actual data production tests from vertical wells from Sabriyah fields in Kuwait to

establish a new generalized multiphase flow choke correlation that predicts liquid flow rates as a function of flowing wellhead pressure, surface choke size and gas-liquid ratio [17].

In 2015, Okon used sixty four (64) field test data from oil producing wells in the Niger Delta region of Nigeria to develop wellhead pressure-production rate correlations based on Gilbert and modified Gilbert equations [18]. The developed equation is given by:

$$P_{WH} = \frac{5.1474q_1R^{0.5048}}{S^{1.7093}} \tag{4}$$

In 2014, Ebuka used an integrated production model (Prosper software) to optimize production in a mature Niger Delta field where continuous declining rates greatly limited the economics for routine production optimization activities [19]. In 2007, Vidovic and Gluscevic optimized production in geothermal wells by performing system analysis at bottomhole and wellhead nodes [20].

## 2. METHODOLOGY

The method deployed in this work is called “Nodal Analysis”. Nodal Analysis involves breaking the system into nodes (characteristic points like tubing, wellhead, choke, etc.) in order to study the performance of the well with reference to fluid flow variables (pressure, flow rate) at the nodes.

In this work, production was optimized by using nodal analysis method to select bean size for two oil wells B40 and B50. The following sets of production data variables were acquired from the industry: bean sizes, flow rates, flowing tubing head pressures, flowing tubing head temperatures, reservoir pressures, reservoir temperatures, tubing sizes, well depths, and gas – oil ratios. Pipeline Simulation Module (PIPESIM) software simulator was used to build the models for the two wells using the test production data acquired from the field. Simulation and choke sensitivity analysis was carried out at two nodes of interest: bottomhole ( $P_{wf}$ ) and wellhead ( $P_{wh}$ ) for each of the wells. The sensitivity analysis was done by simulating the different bean sizes with oil flow rates and pressures to study the effect of the bean size on the inflow/outflow curves and the oil production operating points of the wells. The graphs depicting the sensitivity of increasing or decreasing the choke sizes on the inflow and outflow (operating point) were also plotted.

## 3. RESULTS

The results for the bottomhole as well as the wellhead nodal analyses simulated for wells B40 and B50 are as presented below:

Table 4.1 presents the operating points (coordinates of the intersection) of inflow and outflow curves (pressures and corresponding flow rates) for each of the different bean sizes for Well B40 at the bottomhole node.

**TABLE 4.1: WELL B40 BOTTOMHOLE NODAL ANALYSIS OPERATING POINTS**

BEAN SIZE (inches)	PRESSURE AT NA POINT (psia)	LIQUID FLOWRATE AT NA POINT (STB/D)
0.20	4013.605	415.957
0.25	4000.000	685.824
0.28	3959.732	728.436
0.30	3919.463	929.208
0.40	3825.503	1275.978
0.50	3718.121	1685.516
0.70	3625.263	2029.920
0.80	3612.632	2132.306
1.00	3574.737	2271.923
1.50	3566.737	2327.077
2.00	3557.684	2337.769
3.00	3562.105	2365.001

NA – Nodal Analysis

Table 4.2 presents the operating points (coordinates of the intersection) of inflow and outflow curves (pressures and corresponding flow rates) for each of the different bean sizes for Well B40 at the wellhead node.

**TABLE 4.2: WELL B40 WELLHEAD NODAL ANALYSIS OPERATING POINTS**

BEAN SIZE (inches)	PRESSURE AT NA POINT (psia)	LIQUID FLOWRATE AT NA POINT (STB/D)
0.20	958.050	359.535
0.25	971.365	575.171
0.28	959.732	728.019
0.30	945.190	833.668
0.40	860.850	1210.690
0.50	793.960	1496.312
0.70	735.794	1816.209
0.80	724.161	1890.471
1.00	712.528	1970.445
1.50	711.409	2010.432
2.00	709.172	2016.145
3.00	702.461	2021.857

NA – Nodal Analysis

Table 4.3 presents the operating points (coordinates of the intersection) of inflow and outflow curves (pressures and corresponding flow rates) for each of the different sizes for Well B50 at the bottomhole node.

**TABLE 4.3: WELL B50 BOTTOMHOLE NODAL ANALYSIS OPERATING POINTS**

BEAN SIZE (inches)	PRESSURE AT NA POINT (psia)	LIQUID FLOWRATE AT NA POINT (STB/D)
0.20	4394.183	195.648
0.25	4373.602	438.223
0.28	4342.729	705.056
0.30	4332.438	947.631
0.40	4239.821	1796.644
0.50	4136.913	2888.233
0.70	4023.714	4125.366
0.80	3982.550	4464.972
1.00	3941.387	4828.834
1.50	3920.805	5095.667
2.00	3917.207	5107.813
3.00	3910.515	5119.925

NA – Nodal Analysis

Table 4.4 presents the operating points (coordinates of the intersection) of inflow and outflow curves (pressures and corresponding flow rates) for each of the different bean sizes for Well B50 at the wellhead node.

**TABLE 4.4: WELL B50 WELLHEAD NODAL ANALYSIS OPERATING POINTS**

BEAN SIZE (inches)	PRESSURE AT NA POINT (psia)	LIQUID FLOWRATE AT NA POINT (STB/D)
0.20	840.492	500.005
0.25	814.318	790.325
0.28	796.868	983.872
0.30	793.960	1139.784
0.40	738.702	1962.357
0.50	607.830	2882.492
0.70	465.324	3672.018
0.80	427.517	3870.941
1.00	389.709	4085.993
1.50	369.351	4193.518
2.00	365.403	4218.917
3.00	363.535	4220.400

NA – Nodal Analysis

Table 4.5 presents Well B40 flow characteristics at the wellhead node. The flow rate, pressure ratio, category of flow, and flow regime is specified for each of the bean sizes. Any pressure ratio above 0.55 is not desirable because the choke will not operate at critical flow, thus exposing surface equipment to pressure surges and consequent damage.

TABLE 4.5: WELL B40 FLOW CHARACTERISTICS AT THE WELLHEAD NODE

BEAN SIZE (inches)	FLOWRATE (STB/D)	PRESSURE RATIO	CATEGORY OF FLOW	FLOW REGIME
0.20	359.535	0.53233	Critical	Bubble
0.25	575.171	0.52528	Critical	Bubble
0.28	728.019	0.52500	Critical	Bubble
0.30	833.668	0.52500	Critical	Bubble
0.40	1210.690	0.55720	Sub-critical	Bubble
0.50	1496.312	0.56175	Sub-critical	Bubble
0.70	1816.209	0.59726	Sub-critical	Slug
0.80	1890.471	0.66602	Sub-critical	Slug
1.00	1970.445	0.70003	Sub-critical	Slug
1.50	2010.432	0.72576	Sub-critical	Slug
2.00	2016.145	0.80344	Sub-critical	Slug
3.00	2021.857	0.90836	Sub-critical	Slug

Table 4.6 presents Well B50 flow characteristics at the wellhead node. The flow rate, pressure ratio, category of flow, and flow regime is specified for each of the bean sizes. Any pressure ratio above 0.55 is not desirable because the choke will not operate at critical flow, thus exposing surface equipment to pressure surges and consequent damage.

TABLE 4.6: WELL B50 FLOW CHARACTERISTICS AT THE WELLHEAD NODE

BEAN SIZE (inches)	FLOWRATE (STB/D)	PRESSURE RATIO	CATEGORY OF FLOW	FLOW REGIME
0.20	500.005	0.62213	Sub-critical	Huge Liquid
0.25	790.325	0.56220	Sub-critical	Huge Liquid
0.28	983.872	0.52528	Critical	Huge Liquid
0.30	1139.784	0.52528	Critical	Huge Liquid
0.40	1962.357	0.52500	Critical	Huge Liquid
0.50	2882.492	0.52500	Critical	Huge Liquid
0.70	3672.018	0.56220	Sub-critical	Huge Liquid
0.80	3870.941	0.59816	Sub-critical	Huge Liquid
1.00	4085.993	0.67765	Sub-critical	Huge Liquid
1.50	4193.518	0.76041	Sub-critical	Huge Liquid
2.00	4218.917	0.82823	Sub-critical	Huge Liquid
3.00	4220.400	0.94493	Sub-critical	Huge Liquid

Figure 4.1 presents well B40 bottomhole nodal analysis plot of inflow and outflow curves for different bean sizes. As the bean size is increased successively from 0.2” to 3”, the outflow curves shift repeatedly to the right; hence the points of intersection (operating points) also shift to the right. The plot is as shown below:

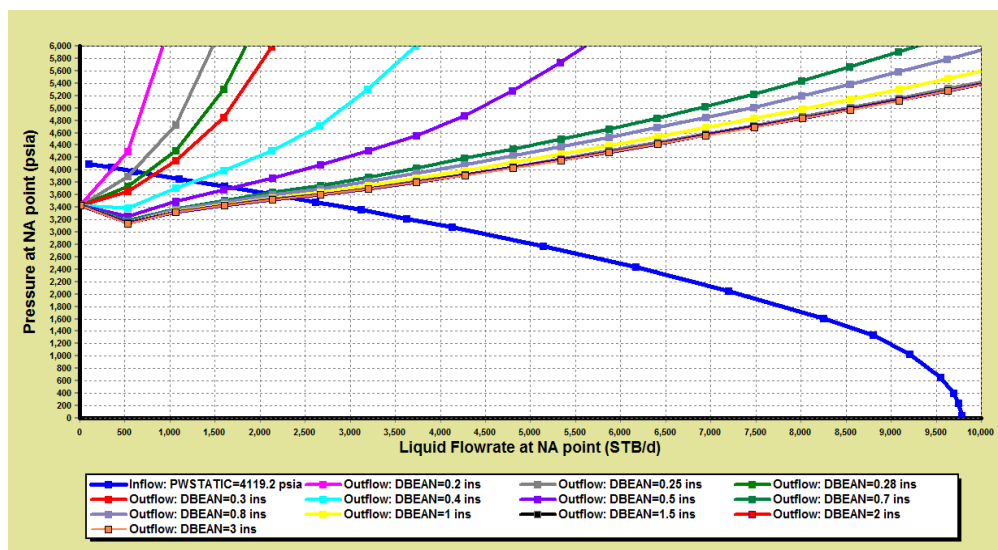


Fig.4.1: Well B40 Bottomhole Nodal Analysis Plot of Inflow and Outflow Curves for Different Bean Sizes

Figure 4.2 presents well B40 wellhead nodal analysis plot of inflow and outflow curves for different bean sizes. As the bean size is increased successively from 0.2” to 3”, the outflow curves shift repeatedly to the right; hence the points of intersection (operating points) also shift to the right. The plot is as shown below:

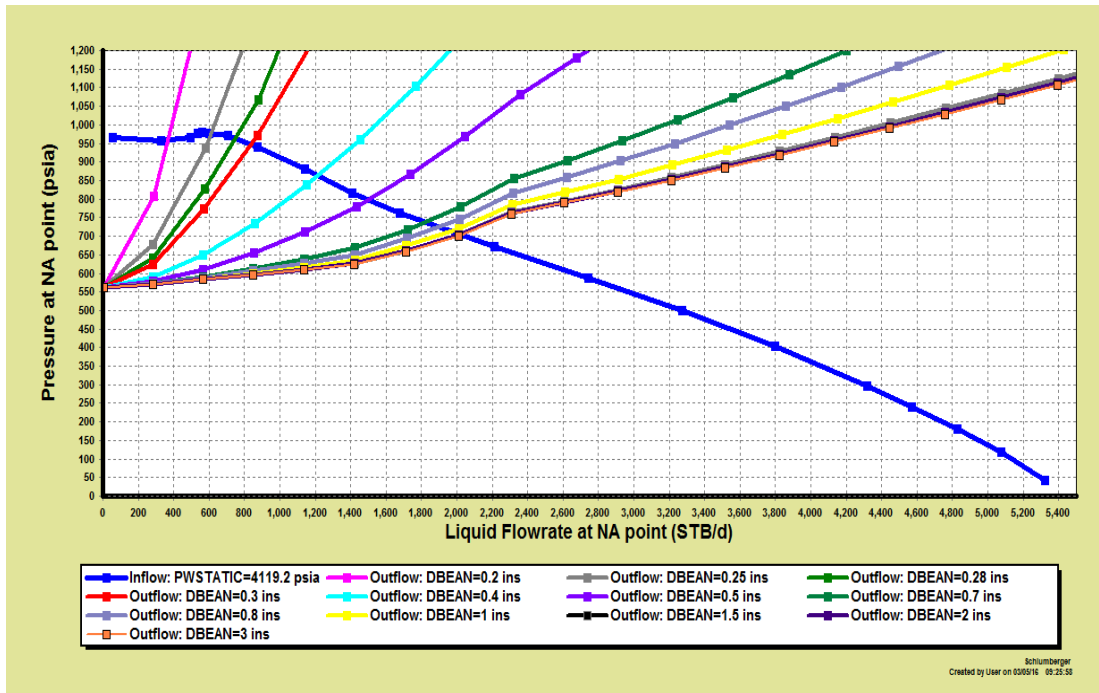


Fig.4.2: Well B40 Wellhead Nodal Analysis Plot of Inflow and Outflow Curves for Different Bean Sizes

Figure 4.3 presents well B50 bottomhole nodal analysis plot of inflow and outflow curves for different bean sizes. As the bean size is increased successively from 0.2” to 3”, the outflow curves shift repeatedly to the right; hence the points of intersection (operating points) also shift to the right. The plot is as shown below:

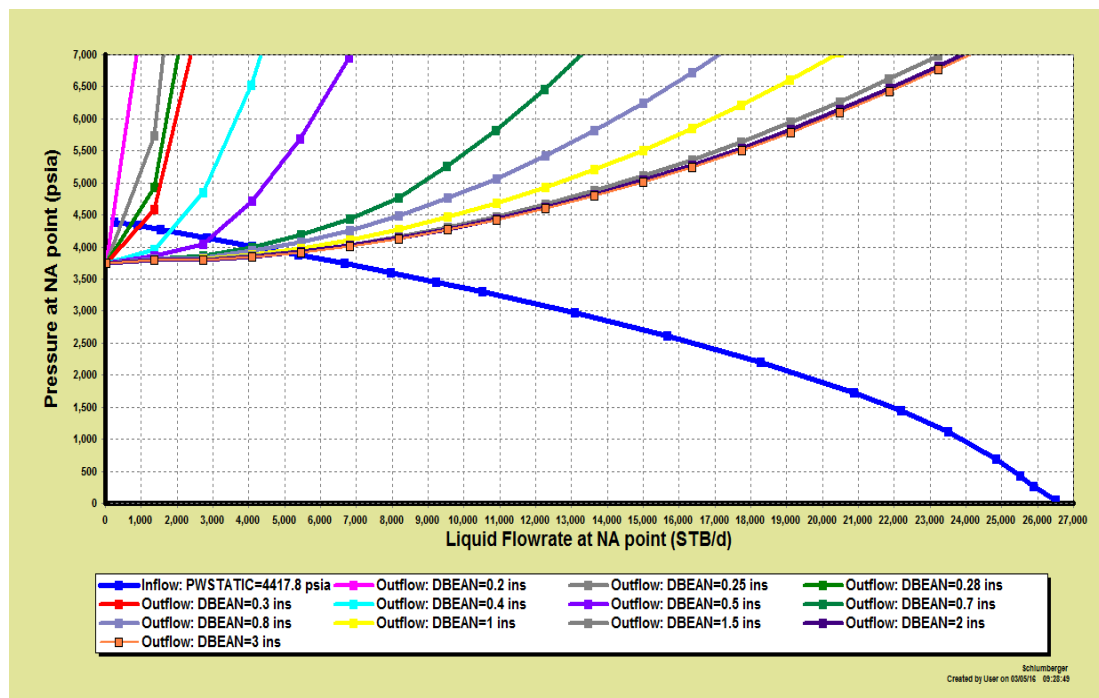


Fig.4.3: Well B50 Bottomhole Nodal Analysis Plot of Inflow and Outflow Curves for Different Bean Sizes

Figure 4.4 presents well B50 wellhead nodal analysis plot of inflow and outflow curves for different bean sizes. As the bean size is increased successively from 0.2” to 3”, the outflow curves shift repeatedly to the right; hence the points of intersection (operating points) also shift to the right. The plot is as shown below:

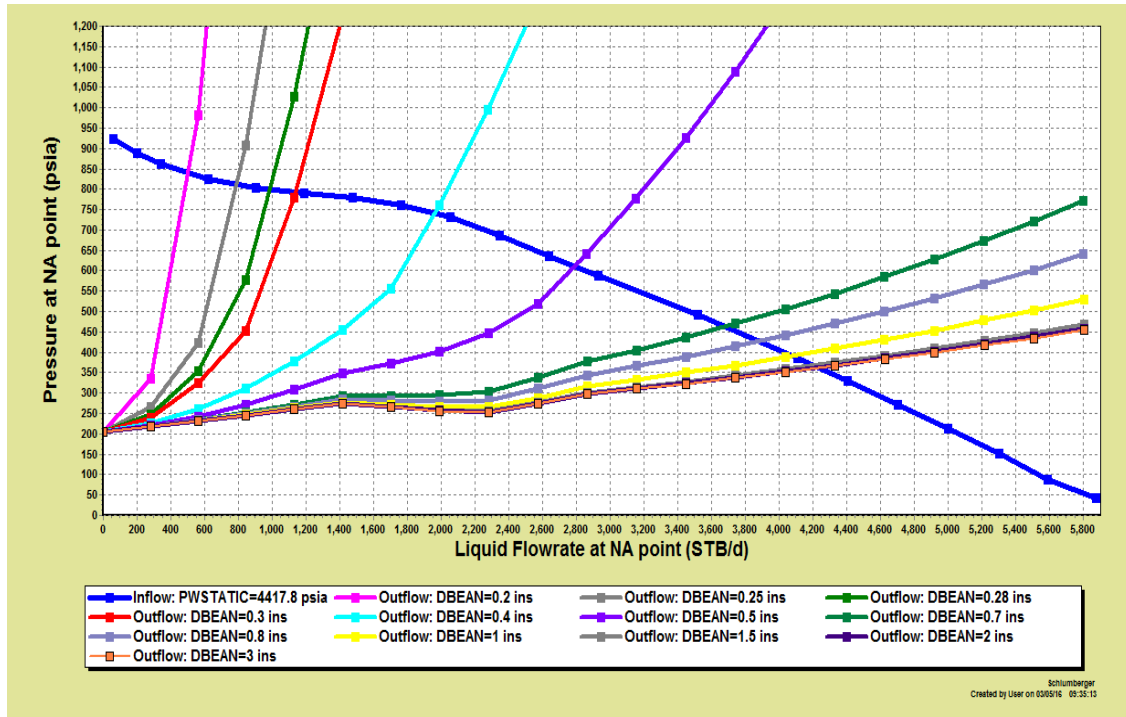


Fig.4.4: Well B50 Wellhead Nodal Analysis Plot of Inflow and Outflow Curves for Different Bean Sizes.

Figure 4.5A presents well B40 combined plots of inflow and outflow curves for both bottomhole and wellhead nodal analyses (different bean sizes). At the optimum bean size, the flow rate at the bottomhole node is the same as the flow rate at the wellhead node. The plot is as shown below:

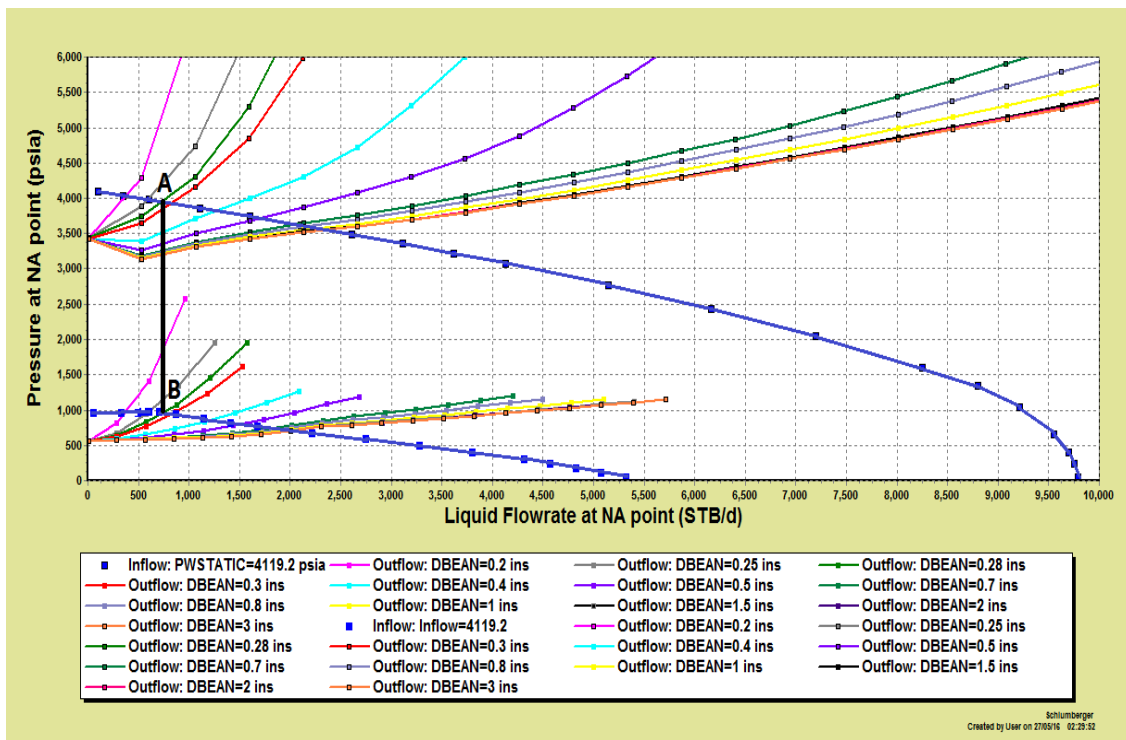


Fig. 4.5A: Well B40 showing combined plots of Inflow and Outflow Curves for both Bottomhole and Wellhead Nodal Analyses (different bean sizes)

Figure 4.6A presents well B50 combined plots of inflow and outflow curves for both bottomhole and wellhead nodal analyses (different bean sizes). At the optimum bean size, the flow rate at the bottomhole node is the same as the flow rate at the wellhead node. The plot is as shown below:

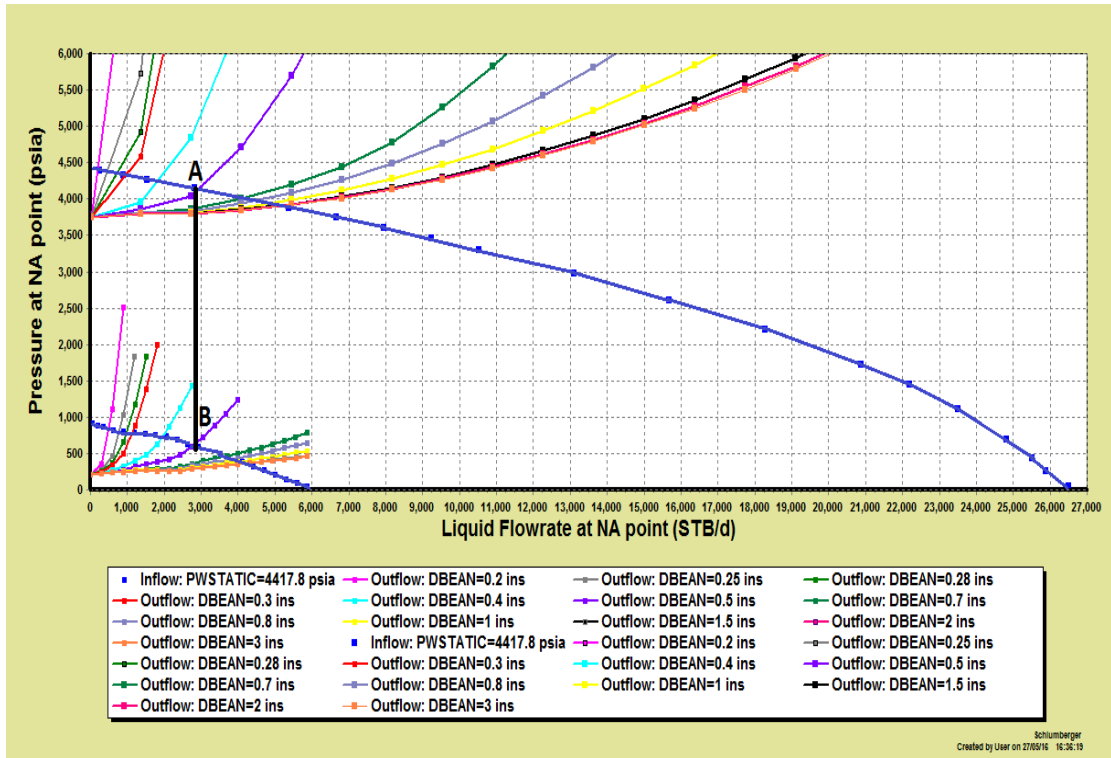


Fig.4.6A: Well B50 showing combined plots of Inflow and Outflow Curves for both Bottomhole and Wellhead Nodal Analyses (different bean sizes)

TABLE 4.7: WELL B40 SHOWING PRESSURE AND FLOWRATE BEFORE AND AFTER OPTIMIZATION

WELL B40	BEAN SIZE (inches)	PRESSURE AT WELL HEAD (psia)	PRESSURE LOSS dP(PSI)	FLOWRATE (STB/D)
BEFORE OPTIMIZATION	0.25 (16/64 or 1/4)	971.365	668.084	605.171
AFTER OPTIMIZATION	0.28 (17.92/64)	959.732	469.928	728.019

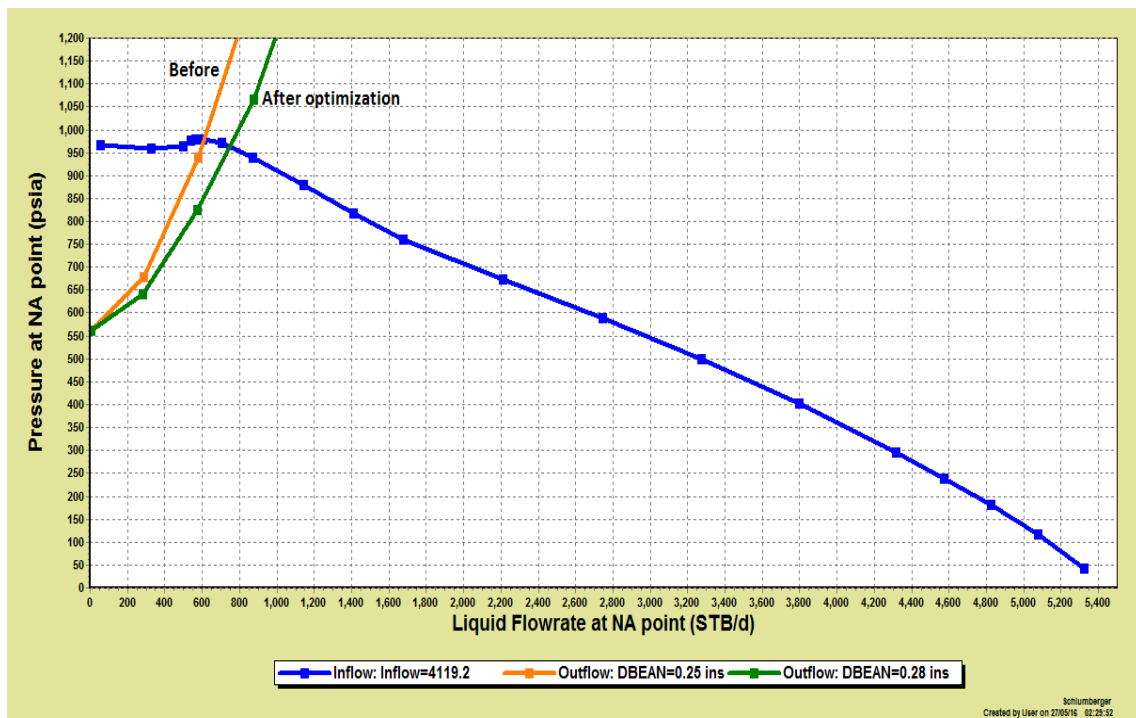


Fig.4.7: Well B40 Nodal Analysis Plot of Inflow and Outflow Curves for initial and optimum bean sizes of 0.25” (before optimization) and 0.28” (after optimization)

TABLE 4.8: WELL B50 SHOWING PRESSURE AND FLOWRATE BEFORE AND AFTER OPTIMIZATION

WELL B50	BEAN SIZE (inches)	PRESSURE AT WH NODE (psia)	PRESSURE LOSS dP (psi)	FLOWRATE (STB/D)
BEFORE OPTIMIZATION	0.40 (25.6/64)	738.702	360.921	1962.357
AFTER OPTIMIZATION	0.50 (32/64 or 1/2)	607.830	303.812	2882.492

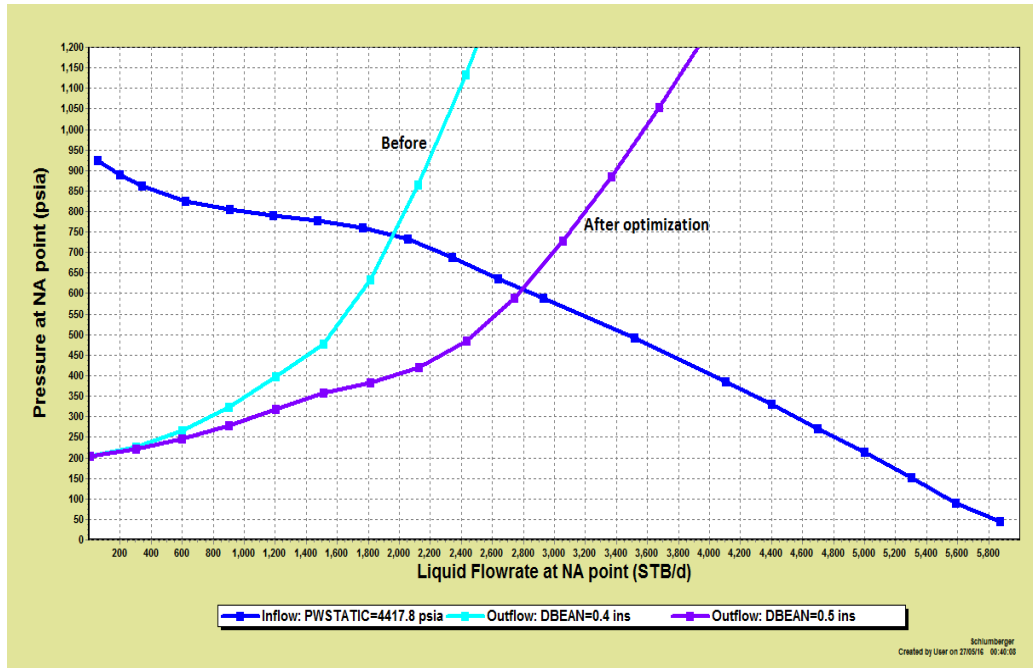


Fig. 4.8: Well B50 Nodal Analysis Plot of Inflow and Outflow Curves for initial and optimum bean sizes of 0.40” (before optimization) and 0.50” (after optimization)

TABLE 4.9: COMPARISON OF RESULTS FOR BEAN SIZE USING DIFFERENT CORRELATIONS

PARAMETERS				RESULTS FOR BEAN SIZE (1/64”)				
WELL	Q (bbl/d)	GOR (SCF/STB)	P <sub>WH</sub> (psi)	SIMULA-TED	GILBERT'S CORR. (EQN 3.5)	BAXENDELL'S CORR (EQN 3.6)	ACHONG'S CORR. (EQN 3.7)	OKON'S CORR. (EQN 3.8)
B40	728.00	543.00	959.80	17.92	18.02	16.57	15.55	14.25
B50	2882.49	148.20	607.50	32.00	32.66	29.67	26.33	28.39

Q – Flowrate; GOR – Gas-oil ratio; P<sub>WH</sub> – Wellhead pressure; CORR. – Correlation; EQN - Equation

#### 4. DISCUSSION

The discussion considers the sensitivity of the oil inflow and outflow rate to changes in the bean sizes of the choke. The deduced results are studied with reference to the functions of pressure maintenance, surface equipment protection, flow rate regulation, and bean up-bean down operations.

The oil inflow and outflow rate analysis was carried out on two oil wells (B40 and B50). Nodal analysis simulated results on two nodes of interest (bottomhole and wellhead) was done to study the sensitivity of the point of coincidence of inflow and outflow rate curves to changes in the bean sizes. This coincident point (which is the intersection of inflow and outflow curves) defines the operating point. This implies that the pressure at the operating point is the optimum for the corresponding flow rate, hence it satisfies the condition. If any change is made either in the inflow or outflow, then only that curve will be shifted and the other will remain the same, but the operating point (intersection) will also change. For this work, the sensitivity analysis was studied by using different bean sizes at the choke.

Tables 4.1 and 4.2 show the well B40 simulated results for the bottom hole and wellhead nodal analyses respectively. The two tables present the coordinates of the intersection of inflow and outflow curves (pressures and corresponding flow rates) for each of the different bean diameters. These points of intersection are the operating points for each of the different bean sizes because the pressures and flow rates at those points satisfy the conditions for well B40.

Similarly, Tables 4.3 and 4.4 show the well B50 simulated results for the bottom hole as well as the wellhead nodal analyses. The two tables present the coordinates of the intersection of inflow and outflow curves (pressures and corresponding flow rates) for each of the different bean diameters. These points of intersection are the operating points for each of the different bean sizes because the pressures and flow rates at those points satisfy the conditions for well B50.

Here the sensitivity analysis was carried out on the outflow by using different bean sizes to study the relationships and variations in the corresponding operating points (pressures and flow rates) to changes in bean sizes. From the tables, it is observed that as the bean size increases, the nodal point pressure reduces while the corresponding flow rate increases. This implies that increasing the bean size results in increased oil production.

In Table 4.1 for well B40 bottomhole nodal analysis, a bean size of 0.20" (12.8/64) produced a flow rate of 363.957STB/d at a pressure of 4013.605psia. However, with a bean size of 0.3" (19.2/64), the pressure is 3919.463psia while the flow rate is 829.208STB/d. As the bean size is further increased progressively to 0.8" (51.2/64), the pressure reduces to 3612.632psia and the corresponding flow rate increases to 2132.306STB/d.

Also, in Table 4.2 for well B40 wellhead nodal analysis, a bean size of 0.20" (12.8/64) produced a flow rate of 359.535STB/d at a nodal point pressure of 958.050psia. However, with a bean size of 0.3" (19.2/64), the pressure is 945.190psia while the flow rate is 833.668STB/d. As the bean size is further increased progressively to 0.8" (51.2/64), the pressure reduces to 724.161psia and the corresponding flow rate increases to 1890.4716STB/d.

Similarly, in Table 4.3 for well B50 bottomhole nodal analysis, a bean size of 0.20" (12.8/64) produced a flow rate of 195.648STB/d at a pressure of 4394.183psia. However, with a bean size of 0.3" (19.2/64), the pressure is 4332.438psia while the flow rate is 947.631STB/d. As the bean size is further increased progressively to 0.8" (51.2/64), the pressure reduces to 3982.550psia and the corresponding flow rate increases to 4464.972STB/d.

Table 4.4 for well B50 wellhead nodal analysis follows the same trend. With a bean size of 0.2", the pressure is 840.492psia while the flow rate is 500.005STB/d. A bean size of 0.3" produces a flow rate of 1139.784STB/d at a pressure of 793.960psi. However, as the bean size is further increased to 0.8", the pressure reduces to 427.517psia and the corresponding flow rate increases to 3870.941STB/d.

Tables 4.5 and 4.6 present Wells B40 and B50 flow characteristics at the wellhead node. The flow rate, pressure ratio, category of flow, and flow regime is specified for each of the bean sizes. Any pressure ratio above 0.55 is not desirable because the choke will not operate at critical flow, thus exposing surface equipment to pressure surges and consequent damage. Sub-critical flow is only desirable at the subsurface conditions.

Figures 4.1 and 4.2 show the plots of well B40 inflow and outflow curves for bottomhole and wellhead nodal analyses respectively. From the two figures, the intersections of inflow and outflow curves (the operating points) are observed to follow a common trend. As the bean size is increased successively from 0.2", the outflow curves shift repeatedly to the right; hence the points of intersection (operating points) also shift to the right. This implies that as the bean size is increased, it causes the operating point to also shift to the right, thus the flow rate increases, indicating that more oil is produced.

Similarly, Figures 4.3 and 4.4 show the plots of well B50 inflow and outflow curves for bottomhole and wellhead nodal analyses respectively. From the two figures, the intersections of inflow and outflow curves (the operating points) are observed to follow the same trend as that of well B40. As the bean size is increased, the outflow curves shift to the right; hence the points of intersection (operating points) also shift to the right, causing the flow rates to increase, and consequently resulting in the production of more oil.

Figure 4.5A shows well B40 combined plots of inflow and outflow curves for both Bottomhole and Wellhead Nodal Analyses (with different bean sizes). These two sets of curves on the same graph show that the intersection (operating points denoted by A and B respectively) with regards to the x-axis (which is the flow rate, denoted by point C) is the same at both bottomhole and wellhead nodal points. From Figure 4.5A, a bean size of 0.28" produced oil at a flow rate of

726.824STB/d. Hence, this quantity of produced fluid or flow rate is the same at both bottomhole and wellhead nodal points, which is in agreement with the mass preservation law which states that “for any system closed to all transfers of matter and energy, the mass of the system must remain constant over time, as the system mass cannot change quantity if it is not added or removed”. Therefore, the optimum bean size for well B40 is 0.28” or 18/64 because it produces 726.824STB/d at both bottomhole and wellhead nodal points, thus obeying the mass preservation law which states that “for any system closed to all transfers of matter and energy, the mass of the system must remain constant over time, as the system mass cannot change quantity if it is not added or removed”.

Similarly, Figure 4.6A shows well B50 combined plots of inflow and outflow curves for both Bottomhole and Wellhead Nodal Analyses (with different bean sizes). These two sets of curves on the same graph show that the intersection (operating points) with regards to the x-axis (which is the flow rate) is the same at both bottomhole and wellhead nodal points. From Figure 4.5A, a bean size of 0.50” (32/64) produced at a rate of 2882.233STB/d. Hence, this quantity of produced fluid or flow rate is the same at both bottomhole and wellhead nodal points, which is in agreement with the mass preservation law. Therefore, the optimum bean size for well B40 is 0.50” or 32/64. Figure 4.6B shows the operating points for the optimum bean size of 0.5” denoted by letters A and B. Point C is the common flow rate of 2882.233STB/d for the two nodal points.

Table 4.7 presents well B40 wellhead nodal point pressure of 971.365psia, a flow rate of 605.171STB/d and a pressure drop of 668.084psi with an initial bean size of 0.25” (16/64) prior to optimization. However, after optimization, the optimum bean size is 0.28” (17.92/64), pressure is 959.732psia at a flow rate of 728.019STB/d and pressure loss of 469.928psi.

Figure 4.7 shows well B40 operating points prior to optimization (point B) and after optimization (point A). The shift from point A to B implies increased production. Similarly, Table 4.8 presents well B50 wellhead nodal point pressure of 738.702psia, a flow rate of 1962.357STB/d and a pressure drop of 360.921psi with an initial bean size of 0.4” (25.6/64) prior to optimization. However, after optimization, the optimum bean size is 0.5” (32/64), pressure is 607.830psia at a flow rate of 2882.4929STB/d and pressure loss of 303.81psi.

Figure 4.8 shows well B50 operating points prior to optimization (point B) and after optimization (point A). The shift from point A to B implies increased oil production from 1962.357bbl/d to 2882.492bbl/d.

Table 4.9 shows the comparison of the bean size results using different correlations. For Well B40, the Gilbert’s correlation (Equation 3.5) gave 18.02”, Baxendell’s correlation (Equation 3.6) gave 16.57”, Achong’s correlation (Equation 3.7) gave 15.55”, and Okon’s correlation (Equation 3.8) gave 14.25”. For Well B50, Gilbert’s correlation gave 32.66”, Baxendell’s: 29.67”, Achong’s: 26.33” and Okon’s: 28.39”. The results gotten from this research are closest to those of Gilbert’s correlation as shown in Table 4.9.

## 5. CONCLUSION

The importance of facilities re-designs (reselection of bean sizes after a period of time) in oil and gas production operations cannot be overemphasized. This is because of effects resulting from a bean size being too small {unstable flowrate, high gas oil ratio (HGOR),  $R_{si}$  greater than 3} or too big (sand and water production). It is therefore imperative to choose an optimum bean size so as to prevent the production of unwanted fluids at the early stage, and to maintain stable deliverability, thus producing the reservoir at the most efficient rate (MER).

The results of the production optimization using bean size selection through nodal analysis method, performed on two oil wells B40 and B50 at both bottomhole and wellhead nodes show that:

1. The flow rate increases with increase in the bean size, which implies that oil production also increases with increased bean size (Tables 4.1, 4.2, 4.3 and 4.4.). In well B40, when bean size is 0.2”, flow rate is 363.957STB/D and 359.535STB/D; when bean size is 0.4”, flow rate is 1275.978STB/D and 1210.690STB/D; when bean size is 0.8”, flow rate is 2132.306STB/D and 1890.471STB/D at bottomhole and wellhead nodes respectively.
2. The operating point (intersection of inflow and outflow curves) shifts repeatedly to the right as the bean size is increased successively (Figures 4.1, 4.2, 4.3 and 4.4).

3. At the optimum bean size, the flow rate at the bottomhole node is the same with that of the wellhead node, thus the law of conservation of mass is obeyed (Figures 4.5A, 4.5B, 4.6A and 4.6B). At optimum bean size of 0.28" for well B40, the flow rate is 728.019STB/D at both bottomhole and wellhead nodes.
4. Nodal point pressures at the bottomhole node are higher in values than those of the wellhead node. This is because of the pressure losses at the vertical section of the tubing. (Tables 4.1, 4.2, 4.3 and 4.4). In well B40, at a bean size of 0.2" the bottomhole pressure is 4013.605psia and wellhead pressure is 958.050psia; at a bean size of 0.5", the bottomhole pressure is 3718.121psia while the wellhead pressure is 793.960psia.

#### REFERENCES

- [1] Ajienska, J. A. and Ikoku, C. U. (1987). A Generalized Model for Multiphase Flow Metering, SPE Paper 17174-MS presented at the Tenth Annual International Conference of Society of Petroleum Engineers held in Lagos, Nigeria, pp. 2 – 6.
- [2] Carroll, J. A. (1990). Multivariate Production Systems Optimization, A Report Submitted to the Department Of Petroleum Engineering and The Committee on Graduate Studies of Stanford University, pp. 4 – 6.
- [3] Nasriani, H. R. and Kalantariasl A. (2011). Two Phase Flow Choke Performance in High Rate Gas Condensate Wells, presented at Society of Petroleum Engineers Asia Pacific Oil and Gas Conference and Exhibition held in Jakarta, Indonesia, pp. 5 - 7.
- [4] Tangren, R. F, Dodge, C. H. and Seifert, H. S. (1949). Compressibility Effects in Two-Phase Flow, *Journal of Applied Physics*, 20(7): 637 - 645.
- [5] Ros, N. C. J. (1960). An Analysis of Critical Simultaneous Gas/liquid Flow through a Restriction and its Application to Flow Metering, *Applied Science Research*, 9(1): 374–388.
- [6] Poettmann, F. H. and Beck, R. L. (1963). New Charts Developed to Predict Gas-Liquid Flow through Chokes, *World Oil* (March 1963), pp. 95-101.
- [7] Omana, R, Houssiere, C. Jr, Brown, K. E, Brill, J. P, and Thompson, R. E. (1969). Multiphase Flow through Chokes, SPE Paper 2682 presented at the 44<sup>th</sup> Society of Petroleum Engineers Annual Meeting held in Denver, Colorado on September 28 – October 1, pp. 9 - 14.
- [8] Ashford, F. E. and Pierce, P. E. (1975). Determining Multiphase Pressure Drops and Flow Capacities in Down-hole Safety Valves, *Journal of Petroleum Technology*, (September), 27(1): 1145 - 1152.
- [9] Gilbert, W.E. (1954). Flowing and Gas-Lift Well Performance. *API Drilling and Production Practice*, 143(1): 126 - 157.
- [10] Baxendall, P. B. (1957). Bean Performance--Lake Wells, *Internal Report* (October), pp.4 – 8.
- [11] Achong, I. (1961). Revised Bean Performance Formula for Lake Maracaibo Wells, *Shell Internal Report* (October), pp. 13 – 17.
- [12] Fortunati, F. (1972). Two Phase Flow through Wellhead Chokes, SPE Paper 3742 presented at the Society of Petroleum Engineers European Meeting, Amsterdam, May 17 – 18, pp. 14 – 19.
- [13] Sachdeva, R, Schmidt, Z, Brill, J. P. and Blais, R. M. (1986). Two-Phase Flow through Chokes, SPE Paper 15657, presented at the Society of Petroleum Engineers 61st Annual Technical Conference and Exhibition, New Orleans, October 5 – 8, pp. 1 – 12.
- [14] Ajienska, J. A. (2005). Christmas Tree, Tree of Life, Tree of Knowledge. An Inaugural Lecture Series No. 47, University of Port Harcourt, Rivers State, December 15, p. 47.
- [15] Elgibaly, A. A. M. and Nashawi, I. S. (1996). Prediction of Two-Phase Flow through Chokes for Middle – East Oil Wells. SPE Paper 36274 presented at 7<sup>th</sup> Abu Dhabi International Society of Petroleum Engineers Exhibition and Conference held at Abu Dhabi, United Arab Emirate, October 13 – 16, p.12.

- [16] Ghareeb, M. and Shedid, A. S. (2007). A New Correlation for Calculating Wellhead Production Considering Influences of Temperature, GOR, and Water-Cut for Artificially Lifted Wells, International Petroleum Technology Conference, Dubai, United Arab Emirate, pp. 23 - 27.
- [17] Alrumah, M. K. and Bizanti, M. S. (2007). New Multiphase Choke Correlations for Kuwait Fields, SPE Paper 105103-MS presented at the Society of Petroleum Engineers Middle East Oil and Gas Show and Conference held in Manama, Kingdom of Bahrain on March 11 – 14, pp. 1 – 4.
- [18] Okon, A. N, Udoh, F. D. and Appah, D. (2015). Empirical Wellhead Pressure-Production Rate Correlations for Niger Delta Oil Wells, SPE Paper 178303-MS, presented at the SPE Nigeria Annual International Conference and Exhibition held in Lagos, Nigeria on August 4 – 6, pp. 2 - 8.
- [19] Ebuka, U. G, Egelle, E, and Ogbunude, B. (2014). Integrated Production Systems Optimization: A mature Niger Delta Field Case Study. International Journal of Science and Research (IJSR) Volume 3 Issue 8, August 2014.
- [20] Slobodan Vidovic and Andreja Gluscevic. (2007). Optimization of Geothermal Wells and Production Systems, Proceedings European Geothermal Congress, Unterhaching, Germany. 30 May-1 June, pp. 1 – 3.